Error reduction for an inertial-sensor-based dynamic parallel kinematic machine positioning system

To cite this article: J Gao *et al* 2003 *Meas. Sci. Technol.* **14** 543

INSTITUTE OF PHYSICS PUBLISHING MEASUREMENT SCIENCE AND TECHNOLOGY

Meas. Sci. Technol. **14** (2003) 543–550 PII: S0957-0233(03)57161-2

Error reduction for an inertial-sensor-based dynamic parallel kinematic machine positioning system

J Gao[1], **P Webb and N Gindy**

School of Mechanical, Materials, Manufacturing Engineering and Management,
The University of Nottingham, University Park, Nottingham NG7 2RD, UK

E-mail: Jian.Gao@nottingham.ac.uk

Received 5 December 2002, accepted for publication 26 February 2003
Published 21 March 2003
Online at stacks.iop.org/MST/14/543

Abstract

This paper addresses the development of an error reduction strategy for an inertial-sensor-based system for measuring the displacement of parallel kinematic machine (PKM) struts and hence the tool centre point pose. The error reduction strategy can significantly improve the performance of low-cost accelerometers and has many potential generic inertial measurement applications.

Inertial measurement systems are prone to errors introduced by manufacturing error, system set-up error and environmental factors. To accurately measure displacement the errors and noise contaminating the inertial data must be removed. Based on data analysis, methods are developed in this paper to remove bias error, and correct integration error through band limitation, error modelling and velocity reconstruction. The velocity reconstruction algorithm described significantly improves the performance of the system and is novel in its use of the bounded nature of the strut displacement. The inertial measurement system described is evaluated using a single PKM-Strut test bed for linear movement and the experimental results are presented and analysed.

Keywords: parallel kinematic machine (PKM), tool centre point (TCP) measurement, inertial sensors, bias error model, low-pass filtering, velocity reconstruction, error reduction

(Some figures in this article are in colour only in the electronic version)

1. Introduction

A parallel kinematic machine (PKM) consists of a number of links, or struts, connected together at the top and bottom by two platforms. If the lengths of the links are varied then the positions of the two platforms will change relative to each other. A PKM potentially possesses considerable inherent advantages compared to traditional (serial link) machine tool structures, as they are more rigid, more agile and can be positionally much more accurate [1].

The key to a PKM's positional accuracy is the precision to which the lengths of the individual parallel links (or struts) can be measured. The struts usually comprise a ball screw and a DC servomotor. The strut length can be measured by a laser interferometer to achieve a high degree of precision [2] but this is expensive. Alternatively, encoders may be mounted on either the motor shaft or on the ball screw and used to measure the relative change in length. Both can only measure ball screw rotation and neither can measure any deformation of the structure caused by mechanical effects such as backlash, wear and thermal expansion which can result in inaccuracies in strut length measurement. These strut length errors will be propagated to the position of the TCP (tool centre point) through the forward kinematic model with a resulting decrease in positional accuracy.

[1] Author to whom any correspondence should be addressed.

Table 1. The linear measurement system specifications.

Specifications	
Accelerometer	
Acceleration range	± 2 g
Zero g output	2.5 V
Resolution	140 μg
Frequency response	0–300 Hz
Transverse sensitivity	<1%
Sensitivity	1000 mV/g
Sampling frequency	1000 Hz
Static linear accuracy	>0.62 mm
Dynamic linear accuracy	>2.5 mm
A/D converter	16 bit resolution

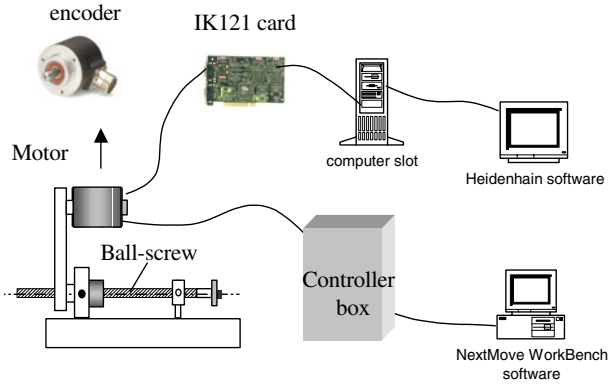

Figure 1. Experimental set-up for the performed encoder measurement.

Inertial sensors such as accelerometers and gyroscopes are widely used in navigation systems to provide vehicle guidance information. They have also been applied to industrial robot applications [3] and machine tool calibration [4]. Ring-laser-gyro inertial sensors have been used to calibrate machine tools at the Honeywell Technology Centre, allowing their systematic errors to be determined and compensated for during normal machining operations. For machine tool applications inertial sensors have the advantage that they directly measure acceleration and can therefore provide the system with dynamic information, such as machine backlash and vibration, which cannot be picked up by a shaft or motor encoder measurement.

The accuracy required for machine tool applications is far higher than that required for pure navigation, and therefore high-grade inertial sensors are normally used [4]. In the past the high cost of inertial systems has seriously limited their practical applications in industrial robots and machine tools. Recent developments in solid-state accelerometers and gyroscopes have resulted in the availability of low-cost sensors that can provide valuable information in many positioning applications if suitable data processing methods are used and external correction is adopted [5]. This paper describes the development of a dynamic displacement measurement system using inertial technology. It also considers the measurement errors and the achievable positional accuracy, and describes the development of data processing methods to improve their performance. Experimental results are presented and analysed.

2. Accelerometer and experimental set-up

The system proposed in this paper is designed to improve the positional accuracy of a PKM through the use of inertial sensors. A typical PKM, such as the Giddings and Lewis Variax, has a maximum acceleration of 2 g, and also has zero acceleration during constant-velocity movements. So the required acceleration range for the inertial measurement system is from DC to 2 g. For the system described in this paper a Kistler 8304B2 single-axis accelerometer with a 0–2 g measurement range was selected for this application [6]. This was combined with a 16-bit A/D converter card. Table 1 summarizes the specification of the inertial measurement system. The signal processing and error correction algorithms were realized using the Matlab environment.

The PKM-Strut prototype system used as a test bed in the application was designed and manufactured at the University of Nottingham as the first step towards the design of a PKM machine tool. The structure of the PKM-Strut contains the mechanical system and control system which includes the motor, control card and servo amplifier. The encoder measurement (position or velocity) in the PKM-Strut test bed was obtained through a Heidenhain IK121 counter card which has an accuracy of 35 μm for linear movement. The experimental set-up for the PKM-Strut measurement system is illustrated in figure 1.

Based on the sensor's frequency response range, the maximum usable sampling frequency of the inertial system is 600 Hz, but a sampling frequency of 1 kHz was used in this application in order to improve the waveform integration accuracy of the measured data.

3. Error analysis and error reduction

Due to manufacturing error, system set-up error and environmental factors, inertial measurement systems experience biases, scale factor errors, noise and other random effects. Errors in the sensed measurement are processed in the same algorithms as the error-free component of the sensor output. These errors build up over time, corrupting the accuracy of the measurement data. Even the slightest offset errors can cause extreme position errors. The error model used to compensate for these errors is described in this section. In the complete system Kalman filtering is used to fuse the inertial data with external measurements to correct the remaining errors and curb the inherent error drift problem of an inertial system, which is introduced in [6].

3.1. System error analysis

Inertial sensor systems are characteristically inaccurate due to a variety of errors. The errors contaminating the signal of interest can be categorized into three types:

- inertial sensor errors, including sensor bias error, cross-axis coupling and scale factor error;
- misalignment error—due to the misalignment angle along the sensitive axis an gravity acceleration component will be sensed as a part of acceleration;
- computational process errors, such as numerical integration error.

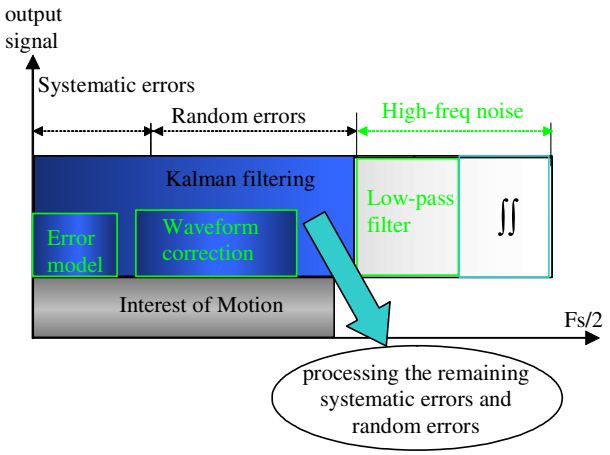

Figure 2. Inertial system error components and corresponding error reduction (Fs—sampling frequency).

In addition to these errors, the dynamic environment within which the inertial sensor is operated affects the way in which these error sources propagate into inertial system errors. Therefore, in the application described here the measured accelerometer data contain wide-bandwidth frequency components, which include the signal of interest, sensor error, environmental noise, machine tool working vibration and instrument circuit electronic noise. These errors are classified as random and systematic errors. Figure 2 shows the error components present in the inertial system and the corresponding data processing methods used.

According to the error source analysis [6], the general error equation used for the accelerometer measurements along the x-axis direction, for example, can be written as

$$\delta a_x = b_a + s_{sf} a_x + s_y a_y + s_z a_z + w, \tag{1}$$

where b_a is the residual measurement biases of the accelerometer; s_{sf} is the scale factor term for the accelerometer; s_y, s_z represents cross-axis coupling factors which depending on the mounting and internal misalignments and w is random noise and vibration in the sensor signal.

In general, the accelerometer bias, cross-axis coupling and scale factor error coefficients can be measured by long-term observation or obtained from the product supplier. Corrections can be made for the repeatable error components. For example, the misalignment error, once the sensor is mounted on the test platform, can be measured and compensated for [6]. Some errors are not constant all the time; bias error for instance is temperature dependent and has switch-on to switch-on variations, and scale factor error is also temperature dependent. Noise and vibration are also variable within dynamic environments. These random errors are less predictable, and therefore cannot easily be compensated for.

In this application, the accelerometer is used to record machine motion and it is that which produces the signal of interest. Due to the low-frequency range of the motion signal, any high-frequency noise present can be filtered using a low-pass filter. Figure 3 shows the accelerometer signal in the time and frequency domain sampled at 1 kHz. The two peaks around 160 and 270 Hz represent the vibration, or noise signal, when the machine was moving. In order to keep the signal

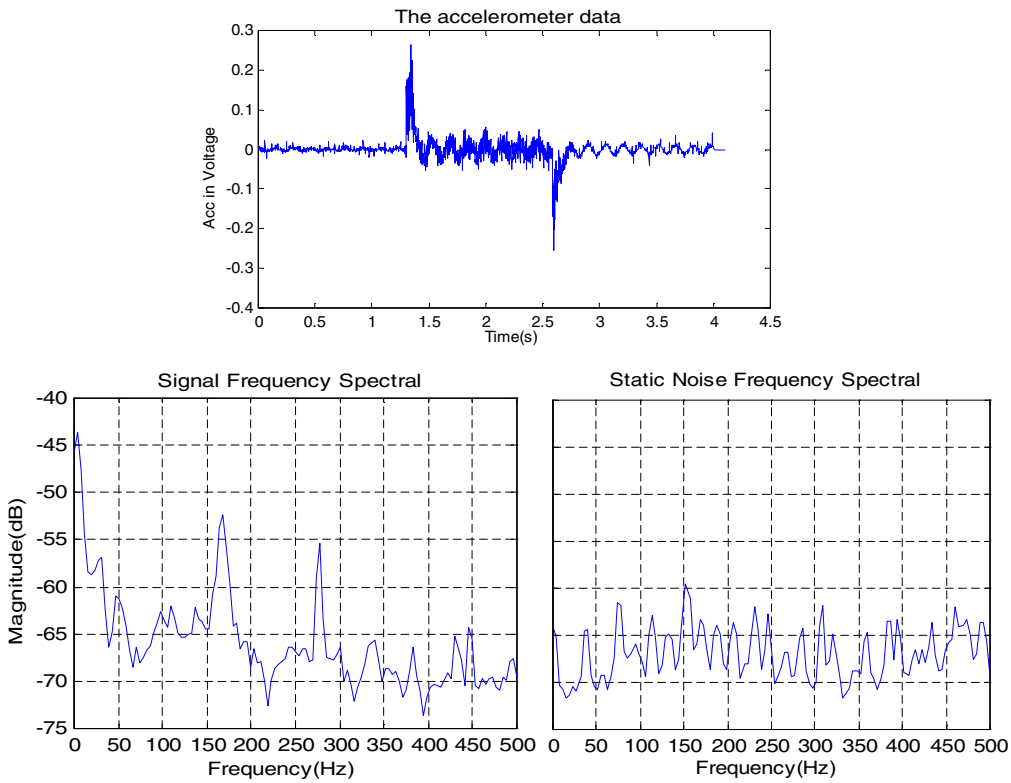

Figure 3. The measured accelerometer data on the test bed.

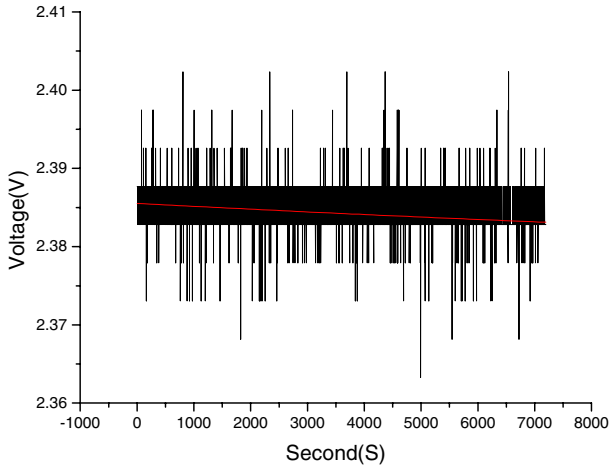

Figure 4. Two hours zero-input measurement by sampling every second for the 8304B2 accelerometer.

unchanged for further processing, an FIR low-pass filter with a cut-off frequency well above the signal of interest was used. In addition to this the double numerical integration performed to derive the displacement result from the measured acceleration also suppresses high-frequency noise.

Two specific approaches are used to remove accelerometer bias error and correct the computational error these are introduced in the following sections.

3.2. Bias error modelling

Accelerometer bias error is one of the important factors in decreasing the system accuracy. A model was therefore constructed to remove this error. For the accelerometer used, the output for zero input would ideally be a constant voltage of 2.5 V, according to the calibration information for the sensor. But, the real output data is at a lower level than ideal at start-up, and the mean value gradually increases or decreases with time in an exponential trend. To develop a bias drift model to remove the error, the accelerometer data were measured under zero-input over periods of 2 h, this is shown in figure 4. The dynamic measurement range is relatively low but the voltage changes measured were very small and at the limits of the data acquisition system. The data do however provide the long-term trend information required. Letting $y(t)$ be the bias error associated with measuring the true value of the acceleration. A non-linear parametric model of the following form was fitted to the accelerometer data using the Levenberg–Marquardt iterative least squares fit model [5, 7, 8]:

$$y(t) = C_0 + C_1 e^{-\frac{t}{T}} = 2.375\,75 + 0.009\,78e^{-\frac{t}{25\,418.26}}(\mathrm{V}) \quad (2)$$

where $y(t)$ is the fitted bias error model for the accelerometer output when zero input was applied.

The residual from the fitted model is computed as follows:

$$e(t) = a_{output}(t) - y_{model}(t) \quad (3)$$

where t corresponds to each sampling point and $e()$ represents the residual value.

When the trend in the measured data has been subtracted out, the residual data $e(t)$ is assumed to be stationary. It has been proved that the estimated autocorrelations for lags greater than one are small compared with the standard error, so there is no reason to doubt the adequacy of the model $\rho_1 \neq 0$, $\rho_k = 0$, $(k \geqslant 2)$ [9].

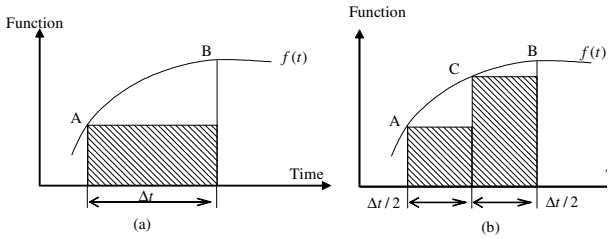

Figure 5. Integration step and error.

3.3. Velocity waveform reconstruction

Even though several methods have been developed to improve the quality of the measured data, not all of the errors in the inertial system can be completely compensated for or removed. The residual error overlaps with the signal of interest and will cause unbounded errors in velocity and position through double numerical integration. This generally gives distorted velocity and displacement drift, i.e., displacement continually increases with time.

Since numerical integration is performed not only on the acceleration data, but also on the derived velocity data, any distortion of the velocity waveform will cause further drift error in position. If the distorted velocity waveform can be corrected before position information is derived, then drift error in position measurement can be prevented. The derived velocity waveforms can be observed and reconstructed according to the physical constraints of the measured motion, that is, initial velocity, initial displacement and terminal velocity equal to zero.

Because the experimental data cannot be expressed as a function, or be well fitted by a polynomial, the velocity and position results cannot be directly derived through functional integration. This means that the integration process must be performed on each point contained within the acceleration data to derive the velocity and displacement data. This can be realized through waveform numerical integration methods, such as cumulative rectangle, trapezoidal and Simpson integration methods.

3.3.1. Integration step and error. For the waveform integration, the propagated inertial system errors were directly proportional to the step length of the integration procedure at the data processing stage. The implication of this result is that within limits, the integration errors will disappear as the step length is reduced to zero. This is illustrated in figure 5 by the trivial integration of the waveform shown. Assuming that the waveform is specified numerically at point A, the simplest numerical integration method (rectangular) is to assume that the curve $f(t)$ is a function over the time interval Δt as illustrated in figure 5(a). The shaded rectangle under the curve is the derived integral value, and the remaining area enclosed by the waveform curve and the rectangle is the associated integration error. If the integration step is halved, then two

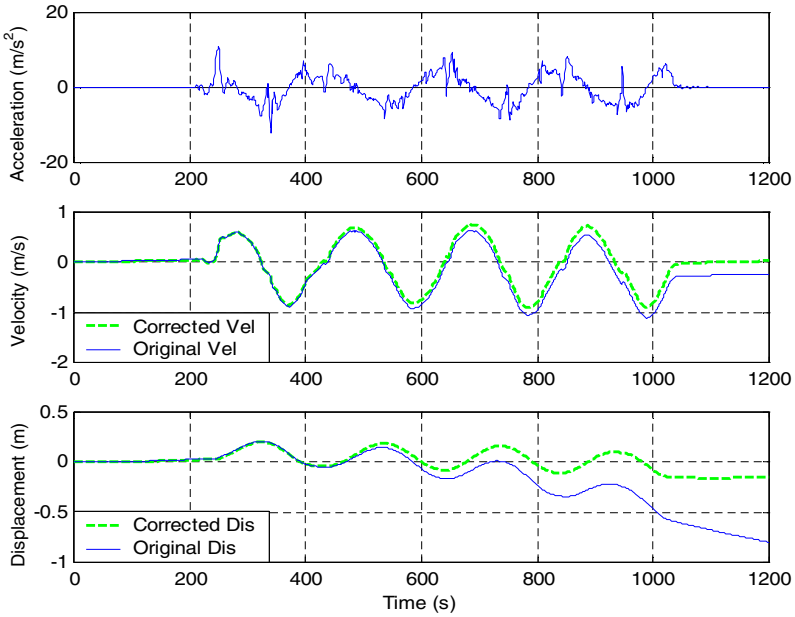

Figure 6. The waveform comparison with and without velocity correction.

calculations for the same area are performed as shown in figure 5(b). It can be seen that the integration error has been halved. If a more accurate integration scheme is selected, then the integration error will be less, but the integration error will still be proportional to the time step. From this point of view, a high sampling rate should be used when data acquisition is performed to reduce the sampling interval and thus reduce the integration error. However, this will result in more noise in the measured data and increase the calculation burden.

3.3.2. Waveform distortion. The integration of the digitized accelerometer data poses an interesting mathematical problem. Due to noise, instrumentation bias and quantization error contaminating the accelerometer data, the resulting velocity and displacement show noticeable non-realistic drifts or distortions. This can be seen from the signal example shown in figure 6. The whole velocity waveform rotates through an angle around the starting point, and the terminal velocity does not return to zero but exhibits an offset. The offset velocity will cause further drifts with time in the derived displacement waveform.

3.3.3. Velocity waveform correction. If the distortion of the velocity waveform can be fitted by a polynomial, then the trend of the waveform distortion can be removed, so as to further reduce integration error in the derived position. Based on a method described by Trujillo and Carter [10], a method of velocity waveform correction was developed in this application using the physical boundary constraints of the machine motion. The constraints are that the initial velocity and displacement when the machine has not started to move yet, and the terminal velocity when the machine has stopped moving, should be zero. This correction approach is only used to reconstruct the velocity waveform, and there is no need to feed it back to the acceleration data, so the algorithm is simple and easy to implement.

According to the physical properties and boundary conditions of machine motion the velocity waveform can be corrected by second-order or first-order polynomials. The correction formula expressed as a second-order polynomial is

$$v_c(t) = v(t) + b_1 t^2 + b_2 t + b_3 \tag{4}$$

then the displacement is

$$x_c(t) = x(t) + \frac{b_1}{3}t^3 + \frac{b_2}{2}t^2 + b_3 t + b_4. \tag{5}$$

From the boundary condition of the machine motion, it has an initial condition when $t = 0$, the initial velocity should be $v_c(0) = 0$, the initial displacement should be $x_c(0) = 0$, and a terminal condition when $t = T$, the terminal velocity should be $v_c(T) = 0$, and the terminal displacement should be $x_c(T) \neq 0$. From formula (5), it is found that the second-order polynomial formula cannot be used to solve the equations because only three conditions are known, and the displacement at the end of the motion is unknown. So the first-order polynomial must be used to fit the waveform trend:

$$v_c(t) = v(t) + b_1 t + b_2 \tag{6}$$

and

$$x_c(t) = x(t) + \frac{b_1}{2}t^2 + b_2 t + b_3. \tag{7}$$

Obtaining the actual value for the initial and terminal condition from the velocity waveform, $v(0), v(T), x(0)$, together with the known boundary condition, $v_c(0) = 0, x_c(0) = 0$ and $v_c(T) = 0$. Substituting them into equations (6) and (7) with $t = 0$ and T gives

$$b_1 = \frac{1}{T}[v(0) - v(T)], \qquad b_2 = -v(0), \qquad b_3 = -x(0).$$

So the velocity correction formula can be expressed as

$$v_c(t) = v(t) + \frac{1}{T}[v(0) - v(T)] - v(0) \tag{8}$$

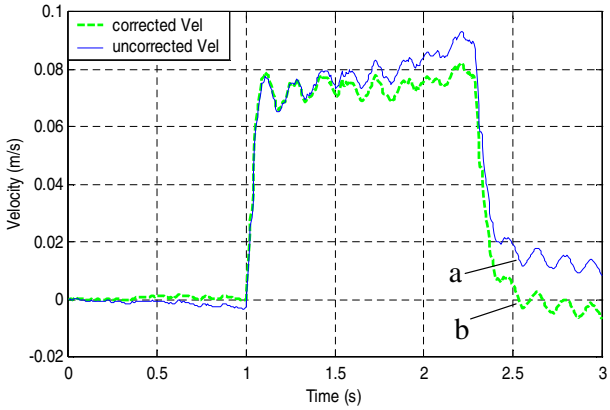

Figure 7. Velocity waveform without and with velocity correction.

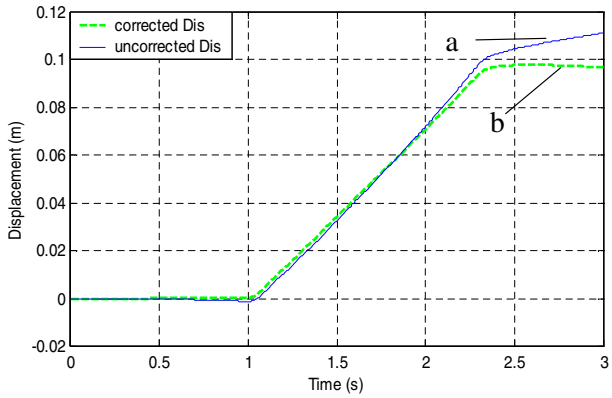

Figure 8. Displacements derived from velocity waveform without and with correction.

$$x_c(t) = x(t) + \frac{1}{2T}[v(0) - v(T)]t^2 - v(0)t - x(0) \qquad (9)$$

where $v(0), v(T), x(0)$ are the values of initial velocity, terminal velocity and initial displacement from the velocity waveform before correction; $v_c(t)$ and $x_c(t)$ are the corrected velocity and displacement at time t.

By applying the method to the signal shown in figure 6, the velocity and displacement curves are corrected as shown. In figure 7, the acceleration data from the test bed were measured; the velocity waveform is corrected (shown in curve b) through the velocity reconstruction. With the corrected velocity waveform, the drifting error in the derived position signal has been effectively removed as shown in figure 8 (curve b). Clearly, the velocity and displacement waveforms can be corrected effectively, and the corresponding errors in velocity and displacement can be reduced. However, the velocity compensation algorithm only operates relative to a discrete point at which final zero velocity is recorded and further drift may occur after this point. The assumption that the final velocity is equal to zero can of course only be made when a measurement of a finite displacement is required. If the system is to be used for continuous feedback then only the initial conditions can be assumed.

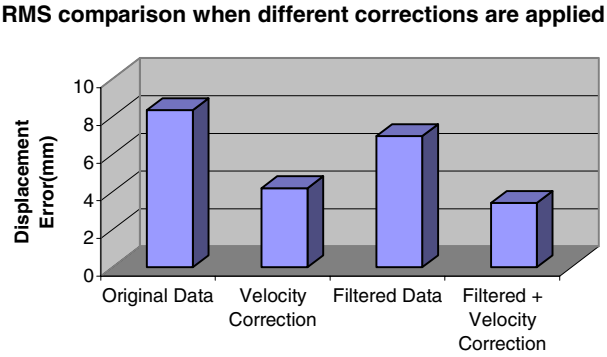

Figure 9. Performance comparisons for a displacement of 100 mm.

4. Results analysis

In the experiments performed, the standard reference displacement was measured by a laser interferometer, whilst the movement of the machine was recorded by the Kistler 8304B2 accelerometer. For a 100 mm movement, the RMS positional accuracy of the displacement error compared with the reference over 20 runs is 8.3 mm without any correction. However, the positional accuracy is improved to 4.2 mm if the velocity waveform correction algorithm was used. This reduces the error by 49% of the uncorrected data. If the velocity waveform correction approach was applied to the velocity waveform derived from the pre-filtered and bias removed acceleration data, then the RMS accuracy is improved to 3.4 mm, a further 19% reduction in the error. Figure 9 shows the performance of the accelerometer data processing with and without the velocity waveform correction and data filtering for a 100 mm movement of machine tool.

In the experiment, the encoder mounted on a machine shaft gives the position information of the ball screw by theoretical calculation, but it cannot measure any dynamic information. The inertial measurement, however, directly measures the dynamic movement of the machine; any vibration, backlash or deformation should be sensed by the accelerometer. So the accelerometer actually measures the real motion of the machine. Through the data processing, the velocity signal derived from the accelerometer measurement is shown in figure 10. The encoder velocity signal and the laser measurement are also shown in figure 10 for comparison. It can be seen that the accelerometer can provide dynamic information that is not present in the encoder velocity information. The laser signal shows a clear 40 Hz oscillation in the motion of the test bed that is not present in the encoder signal. This signal is present in the accelerometer signal but is partially obscured by noise. In the full system this dynamic information is combined with the encoder data using a Kalman filter to provide enhanced velocity and position information [6].

5. Conclusions and discussion

The purpose of the research described in this paper was to develop a low-cost inertial system for the dynamic TCP pose measurement of PKM. The focus of the paper is on inertial system error reduction. Using the methods developed in

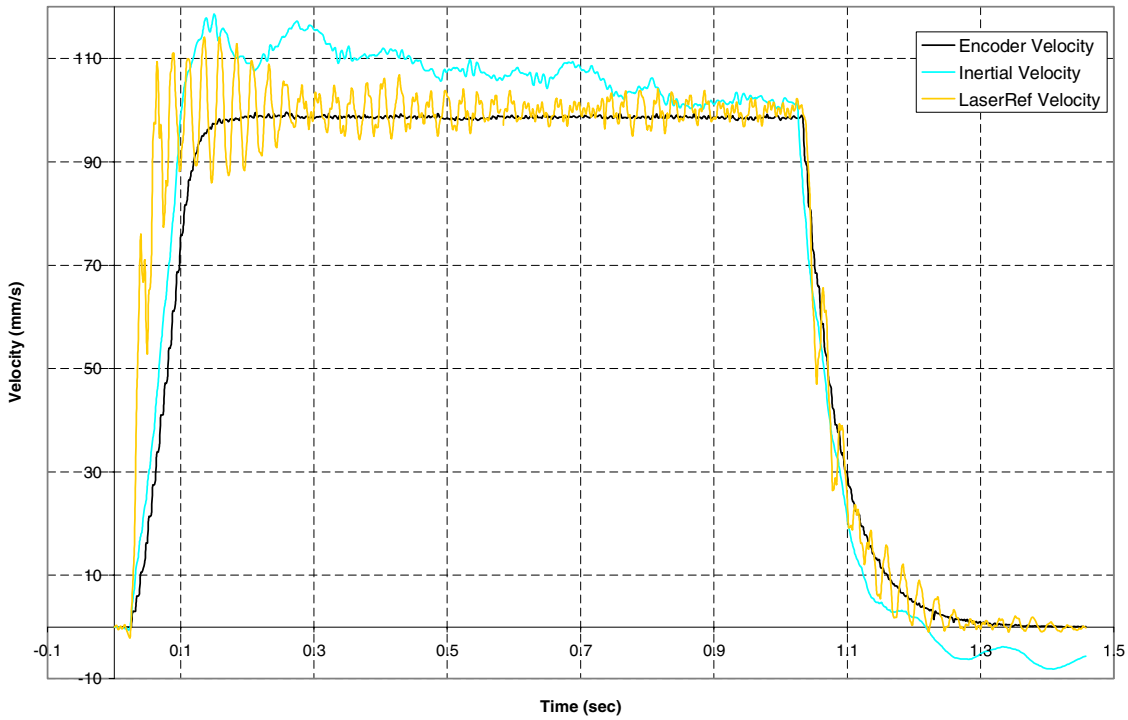

Figure 10. The velocity signal comparison between the accelerometer, encoder and laser measurement.

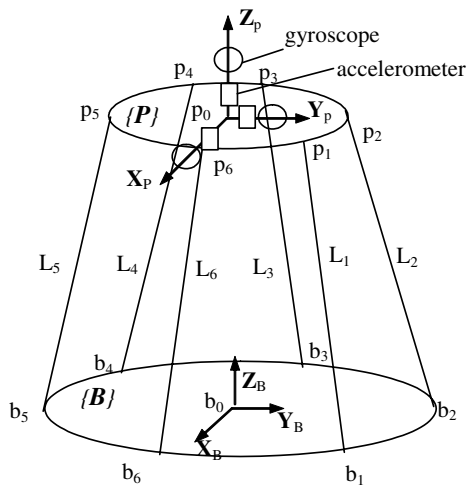

Figure 11. The coordinate systems of a Stewart platform type PKM.

this paper the position error of the inertial system has been reduced by 68% of the position derived from the raw inertial data. Therefore the signal processing methods developed can effectively reduce inertial system error. These methods developed here could also be generally applied to inertial navigation systems. In its basic form the system is better suited to very short duration displacements with return to a known position since the drift error will be relatively small. For long slow displacements and occasions when it is difficult or inconvenient to keep returning to a fixed point then some form of correction must be used

However, compared with the linear position accuracy of 35 μm obtained with the encoder measurement system only, it can be noted that the inertial system accuracy is not good enough to provide the only measurement information. With a further improvement of inertial sensor technology or the employment of a higher-grade sensor, the proposed inertial system could produce a better positional accuracy. The use of high-grade sensor would of course considerably increase the cost of the system to well above that of a linear encoder. The system described does have the inherent advantage that it could be easily mounted at or close to the machine TCP.

However, for a PKM, its kinematics are normally analysed through the inverse kinematic model and forward model. The forward kinematic model cannot be expressed in a closed form solution but only in high-order polynomial equations with one variable. Therefore it is not quite possible to obtain the pose of the PKM–TCP in real time. Some special configurations for the PKM have been proposed to obtain the closed-form solution for the forward kinematic equations [11–16]. These methods depend either on special geometry requirements or on additional sensors and will therefore increase the structure complexity of the machine and affect the limited workspace.

The system described here could be used to directly measure the dynamic motion of the PKM upper platform. If this approach were to be used, an inertial measurement unit (IMU) containing three accelerometers and three gyroscopes could be mounted on the platform and arranged orthogonally to each other (shown in figure 11). The TCP pose of the PKM is derived through the integration of the measured acceleration and angular velocities. Because the TCP has the same pose as the upper platform, except the z-axis value which is calculated by adding the spindle displacement to the platform z value, it was assumed in this application that the pose of upper platform represents the pose of the TCP. Comparing the measured TCP with the ideal TCP, the difference can be sent back to the controller to adjust each leg length through the inverse kinematics model. Figure 12 illustrates the approach

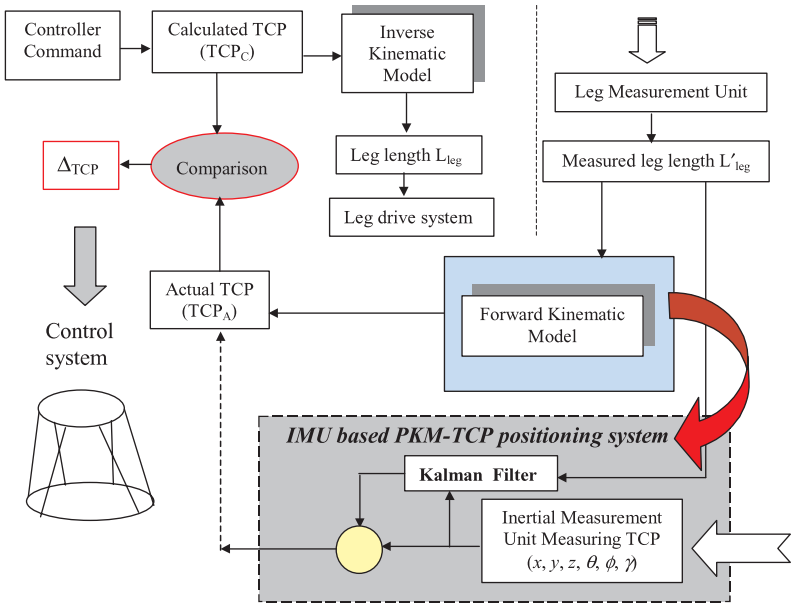

Figure 12. The proposed inertial-sensor-based PKM–TCP positioning system used to directly measure the pose of the TCP.

of the IMU-based PKM–TCP positioning system. Even with the limited accuracy obtained this system could be used to simplify the forward kinematic model through the provision of an approximation of the platform position. In addition, the inertial dynamic measurement can provide dynamic velocity information for the PKM control system. Details on the solution of the PKM pose determination and the system implementation can be referred to [6].

References

[1] Whittingham B D *et al* 1998 Capabilities of parallel link machine tools: preliminary investigations of the Variax Hexacenterä *ASME Int. Mechanical Engineering Congr. Exposition, Anaheim, CA* ed J Lee (New York: ASME)

[2] Soons J A 1997 Error analysis of a hexapod machine tool *Lambdamap'97: 3rd Int. Conf. and Exhibition on Laser Metrology and Machine Performance (July 1997)* pp 347–58

[3] Janocha H and Diewald B 1995 ICAROS: over-all-calibration of industrial robots *Ind. Robot* **22** 15–20

[4] 1994 *Application of Ring Laser Gyros to Precision Machine Tools* (Minneapolis, MN: Honeywell Technology Center)

[5] Barshan B and Durrant-Whyte H F 1995 Inertial navigation systems for mobile robots *IEEE Trans. Robot. Autom.* **11** 328–42

[6] Gao J 2002 Dynamic position sensing for parallel kinematic machine *PhD Thesis* The University of Nottingham

[7] Teukolsky S A and Press W H 1988 *Numerical Recipes in C* (Cambridge: Cambridge University Press) pp 540–7

[8] Barshan B and Durrant-Whyte H F 1998/93 *Inertial Navigation Systems for Mobile Robots* (Oxford: Oxford University Press)

[9] Box G E P and Jenkins G M 1976 *Time Series Analysis: Forecasting and Control* (San Francisco, CA: Holden-Day)

[10] Trujillo D M and Carter A L 1982 A new approach to the integration of accelerometer data *Earthq. Eng. Struct. Dyn.* **10** 529–35

[11] Cheok K C, Overholt J L and Beck R R 1993 Exact methods for determining the kinematics of a stewart platform using additional displacement sensors *J. Robot. Syst.* **10** 689–707

[12] Whittingham B 2001 Applications of the kinematic modelling of a parallel kinematic mechanism machine tool *PhD Thesis* The University of Nottingham

[13] Griffis M and Duffy J 1989 A forward displacement analysis of a class of Stewart platform *J. Robot. Syst.* **6** 703–20

[14] Liu K *et al* 1992 Control of a Stewart-platform-based robotic machining cell *Winter Annu. Mtg ASME Proc. ASME Advanced Control Issues for Robotic Manipulators, ASME Dynamic Systems (Anaheim, CA, Nov. 1992)*

[15] Zhang C and Song S 1991 Forward kinematics of a class of parallel (Stewart) platforms with closed-form solution *Proc. IEEE Int. Conf. on Robotics and Automation* pp 2676–81

[16] Shi X and Fenton R G 1994 A complete and general solution to the forward kinematics problem of platform-type robotic manipulators *Proc. IEEE Int. Conf. on Robotics and Automation* vol 4 pp 3050–62